Supplementary Information for:

A high-throughput screen for acyl-homoserine lactone synthase quorum-sensing inhibitors

Quin H. Christensen[1], Tyler L. Grove[2], Squire J. Booker[2], E. Peter Greenberg[1]*
[1]Department of Microbiology, University of Washington, Seattle, WA 98195, [2]Chemistry, and Biochemistry and Molecular Biology, Pennsylvania State University, University Park, PA 16802

Supplementary Methods

Preparation of apo-ACP. *Escherichia coli* fatty acid apo-ACP was purified from strain JT-apo (Table S1) based on previously published protocols (1–3). Bacteria were grown in 18 liters of 2xYT medium (4) with 15 µg/ml kanamycin, 50 µg/ml streptomycin, 50 µg/ml spectinomycin, and 10 µg/ml chloramphenicol. Acyl carrier protein and AcpH production were induced by addition of 100 µM IPTG and the culture was incubated for 3 to 4 h. Cells were collected by centrifugation (about 100 g of cells wet weight) and stored at -80°C. The frozen cells were thawed and lysed in 100 ml of 100 mM Tris-HCl, 1 mg/ml lysozyme, 0.5 µg/ml DNAse, 1 mM disodium ethylenediaminetetraacetate, 1 mM dithiothreitol, pH 8.0, at 37°C for 20 min (3). The lysate was cleared by centrifugation. We then added $MgCl_2$ and $MnSO_4$ to a final concentration of 25 mM and 1.2 mM respectively. The cleared lysate was then incubated at 37°C for 4 h to convert all ACP to the *apo* form (2). Cellular proteins were precipitated in 50% isopropanol as described (2). ACP was purified from the supernatant fluid by using 60 ml of de-fined Whatman DE23 diaminoethyl cellulose as described (1). Fractions containing pure protein as judged by SDS-PAGE were pooled and precipitated by addition of 0.02% sodium deoxycholate and 5% trichloroacetate as described (2). ACP was suspended in 60 ml of 0.5 M Tris-HCl, pH 8.0. The apo-ACP preparation was dialyzed against 100 mM Tris-HCl, 0.5 mM Tris(2-carboxyethyl)phosphine-HCl, pH 8.0, flash frozen in liquid nitrogen, and stored at -80°C.

Preparation of octanoyl-ACP (C8-ACP). We used *Bacillus subtilis* phosphopantetheinyl transferase, Sfp, to modify apo-ACP with octanoyl-phosphopantetheine to yield C8-ACP as previously described (5). Transferase reactions were in 100 mM Tris-HCl pH 8.0, 10 µM magnesium chloride, 1 mM TCEP with 1 mM apo-ACP, 10 mM C8-CoA, and 10 µM Sfp. Reaction were at 37°C for 3 h after which Sfp was precipitated with ammonium sulfate at 75% saturation for 1 h at 4°C. The precipitate was removed by centrifugation and ACP was precipitated with two volumes of acetone overnight at -20°C. The ACP precipitate was collected by centrifugation, briefly dried, and suspended in 25 mM Tris-HCl pH 7.5, 1mM TCEP. Later procedures are as described in the main text **Materials and Methods**. Modification of ACP was confirmed by mass spectrometry (Fig. S4).

Analysis of screening results. Data from the high throughput screen were processed by using Microsoft Excel and Visual Basic. For all data, percent inhibition is relative to the mean of the DMSO controls. Data from the primary and counter screens were analyzed separately for normality. The data deviated significantly from an ideal Gaussian distribution by the D'Agostino-Pearson test. Skewness was small but kurtosis was 13 and 15 for the primary and counter screen distributions, respectively. This indicates a widening of the tails of the distribution. In contrast, the data could be fit to a Gaussian distribution by nonlinear regression with an R2 >0.99 in each case (Fig. S1).

Analysis of inhibitor IC_{50}. To calculate IC_{50} we used the four-parameter dose-response equation $V=B+(T-B)* [I]H/(IC_{50}H+[I]H)$ where V is the reaction velocity, B is the minimal velocity, T is the maximum velocity, [I] is the log of total inhibitor concentration, IC_{50} is the half-maximal

concentration of inhibitor, and H is the Hill coefficient. V and [I] were known variables and the other terms were unknowns restricted to positive numbers.

K_m and V_{max} analysis. Pseudo first-order kinetic parameters for BmaI1 were determined by measuring enzyme velocity while changing one substrate concentration with the other substrate at a constant concentration. Data were fit to the Michaelis-Menten equation (6). Data are shown in Figure S3.

Supplementary References

1. Rock CO, Cronan JE (1980) Improved purification of acyl carrier protein. *Anal Biochem* 102:362–364.

2. Cronan JE, Thomas J (2009) Bacterial fatty acid synthesis and its relationships with polyketide synthetic pathways. *Methods Enzymol* 459:395–433.

3. Repaske R (1956) Lysis of gram-negative bacteria by lysozyme. *Biochim Biophys Acta* 22:189–191.

4. Miller JH (1972) *Experiments in molecular genetics* (Cold Spring Harbor Laboratory Press).

5. Christensen QH, Cronan JE (2010) Lipoic acid synthesis: a new family of octanoyltransferases generally annotated as lipoate protein ligases. *Biochemistry* 49:10024–10036.

6. Copeland RA (2005) Evaluation of enzyme inhibitors in drug discovery. A guide for medicinal chemists and pharmacologists. *Methods Biochem Anal* 46:1–265.

7. Huson DH et al. (2007) Dendroscope: An interactive viewer for large phylogenetic trees. *BMC Bioinformatics* 8:460.

8. Datsenko KA, Wanner BL (2000) One-step inactivation of chromosomal genes in *Escherichia coli* K-12 using PCR products. *Proc Natl Acad Sci U S A* 97:6640–6645.

9. Duerkop BA, Ulrich RL, Greenberg EP (2007) Octanoyl-homoserine lactone is the cognate signal for *Burkholderia mallei* BmaR1-BmaI1 quorum sensing. *J Bacteriol* 189:5034–5040.

10. Eschenfeldt WH, Lucy S, Millard CS, Joachimiak A, Mark ID (2009) A family of LIC vectors for high-throughput cloning and purification of proteins. *Methods Mol Biol* 498:105–115.

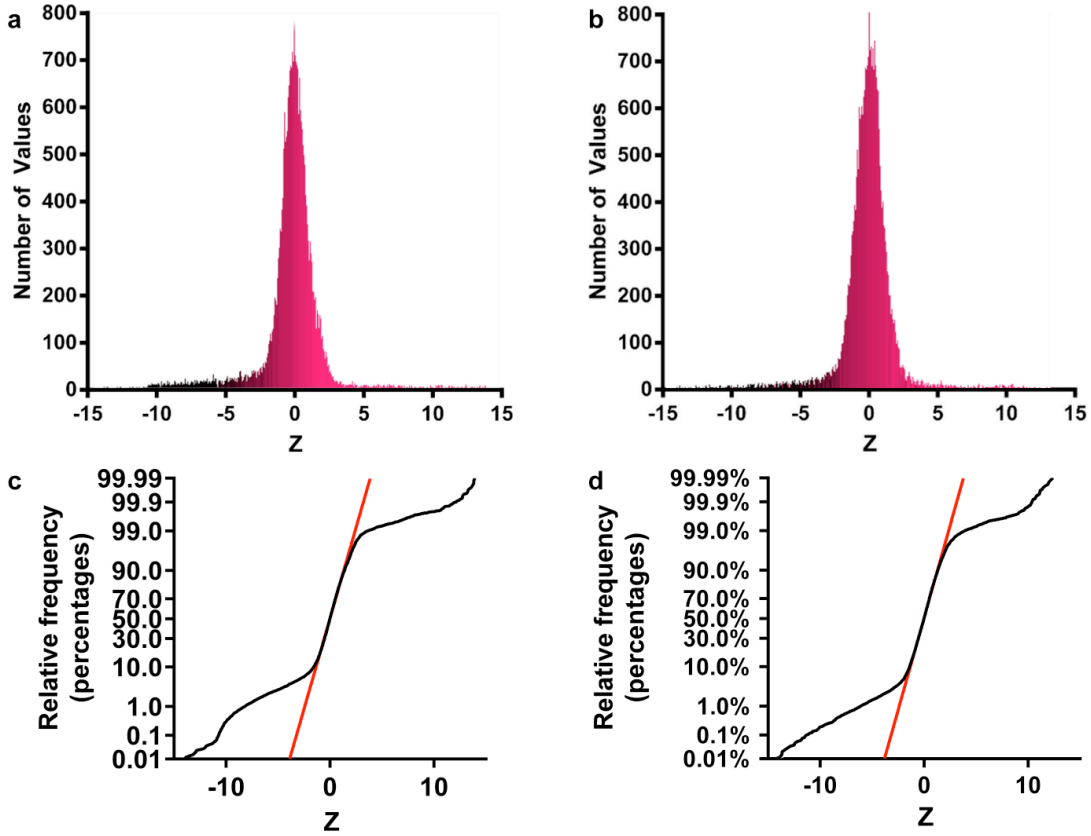

Figure S1: Analysis of primary and counter screen data for normality. Histograms of the combined data from the primary screen (a) and the counter screen (b). The bars are increasingly pink with increasing resorufin concentration. Cumulative frequency distributions are normalized to the maximum value with a percentile Y axis (c and d black lines). The data are fit to an ideal cumulative Gaussian distribution as shown in red. The analysis shows that for both screens >80% of the data conform to an ideal Gaussian distribution but the extreme points deviate from the ideal.

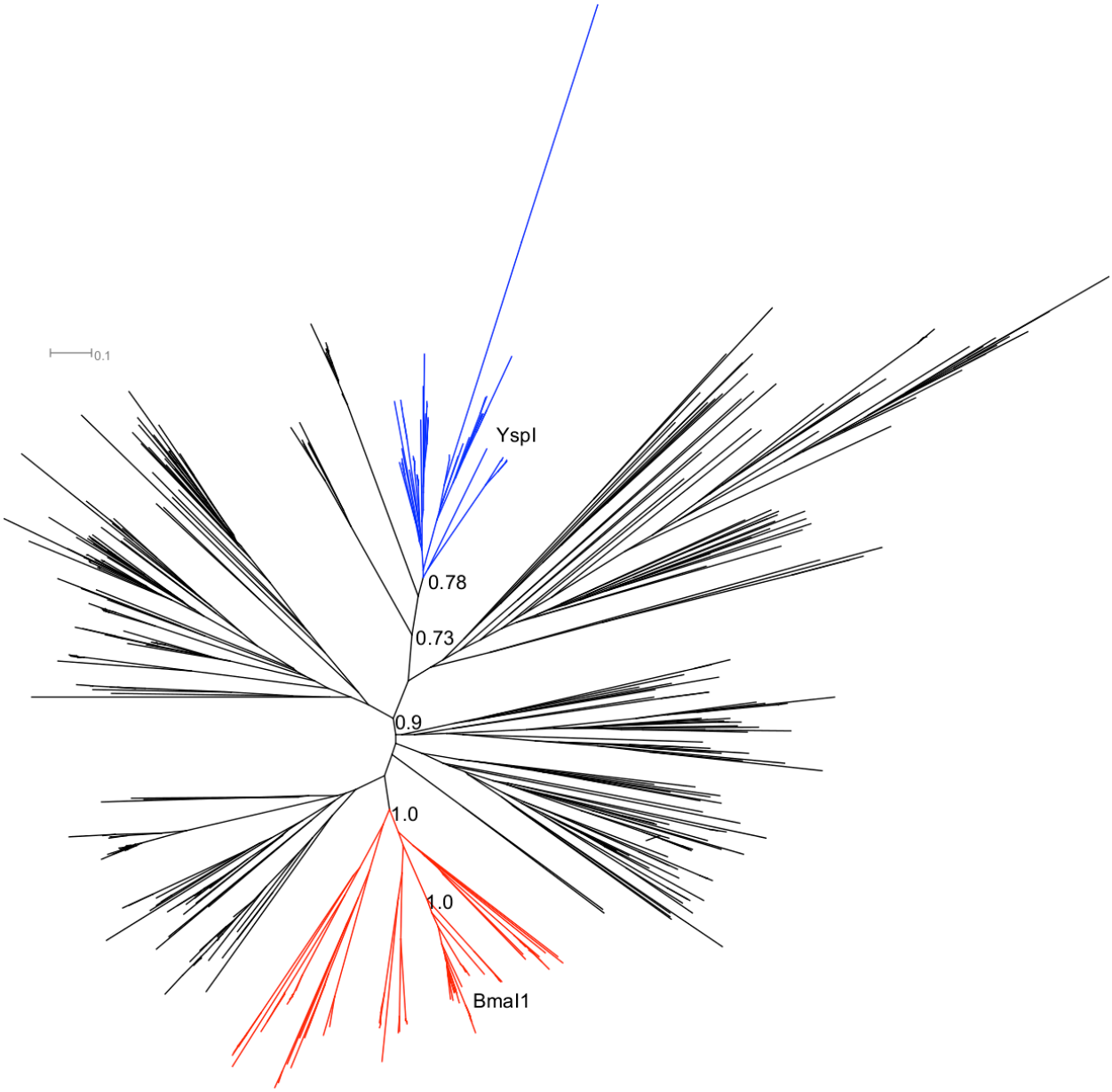

Figure S2: Phylogeny of acyl-HSL synthases in the Uniprot database drawn using Dendroscope (7). The phylogenetic tree of family PF00765 from Pfam is shown. The clades containing synthases from *Yersinia* and *Burkholderia* are highlighted in blue and red, respectively. The bootstrap confidence values for select nodes are indicated; a value of 1 indicates the branch was present in every replicate. The scale bar indicates the number of changes in compared residues per branch length.

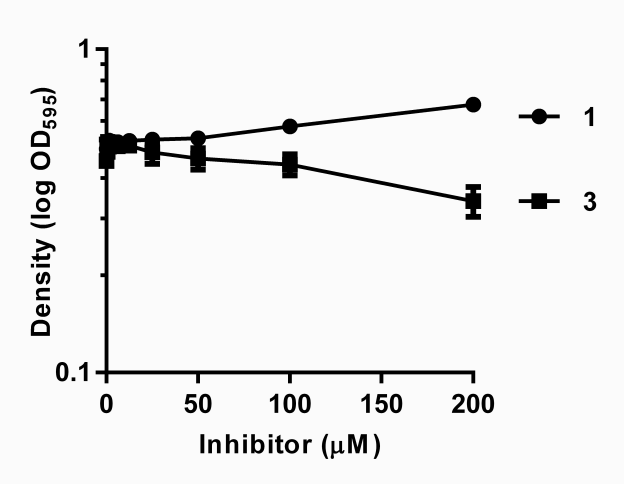

Figure S3: Affects of Bmal1 inhibitors on growth of *E. coli* BW25113 (pBD2). Experiments were according to the Clinical and Laboratory Standards Institute MIC protocol except that we used MOPS minimal medium with 0.4% glucose and 0.4% arabinose. Densities after 20 h at 35°C are shown. The error bars show the standard deviation of four replicates. There was little or no growth inhibition by any of the compounds at any of the concentrations tested. At the highest concentration of compound 1 there was an increase in optical density. We believe this might be a consequence of the poor water solubility of this compound.

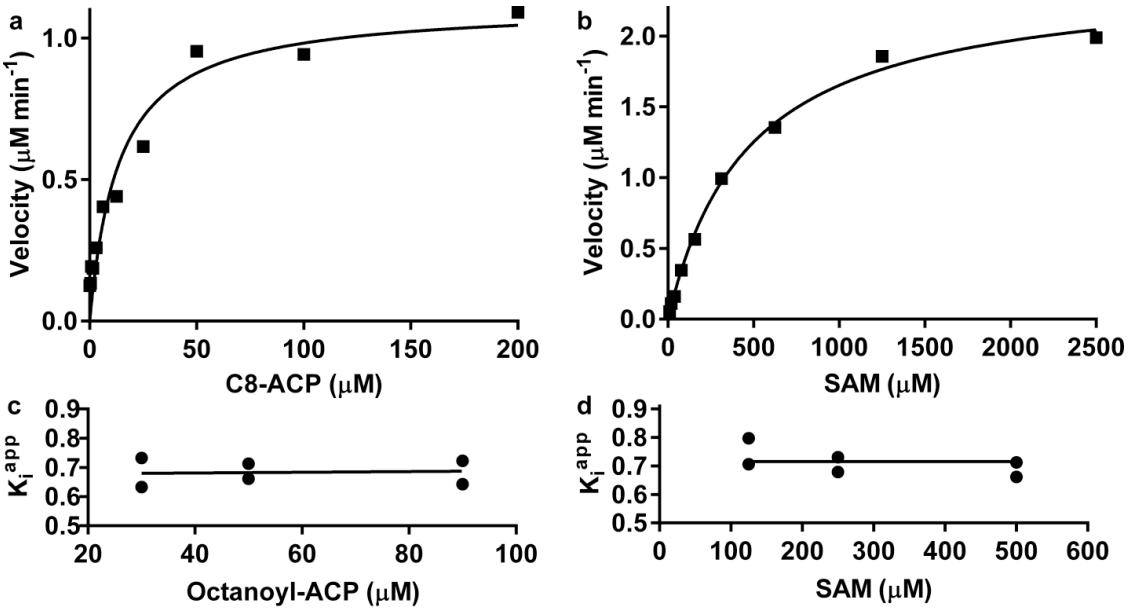

Figure S4: Kinetic analysis of Bmal1 and compound 1. (a) The dependence of the steady-state reaction velocity on the concentration of C8-ACP with 500 μM SAM. Fitting the data to the Michaelis-Menten equation yields an apparent affinity for C8-ACP (K_b) of 14±4 μM and an apparent catalytic constant of 0.037±0.003 s-1. (b) The dependence of the reaction velocity on the concentration of SAM with C8-ACP at 50 μM. Fitting to the Michaelis-Menten equation yields an apparent affinity for SAM (Ka) of 471±39 μM and an apparent catalytic constant of 0.081±0.002 s-1. The substrate dependence of K_i^{app} was determined by using different concentrations of (c) C8-ACP and (d) SAM. Data from both (c) and (d) were simultaneously fit to ideal inhibition models as described in the main text **Materials and Methods**. The data best fit a noncompetitive model, which is shown by black lines.

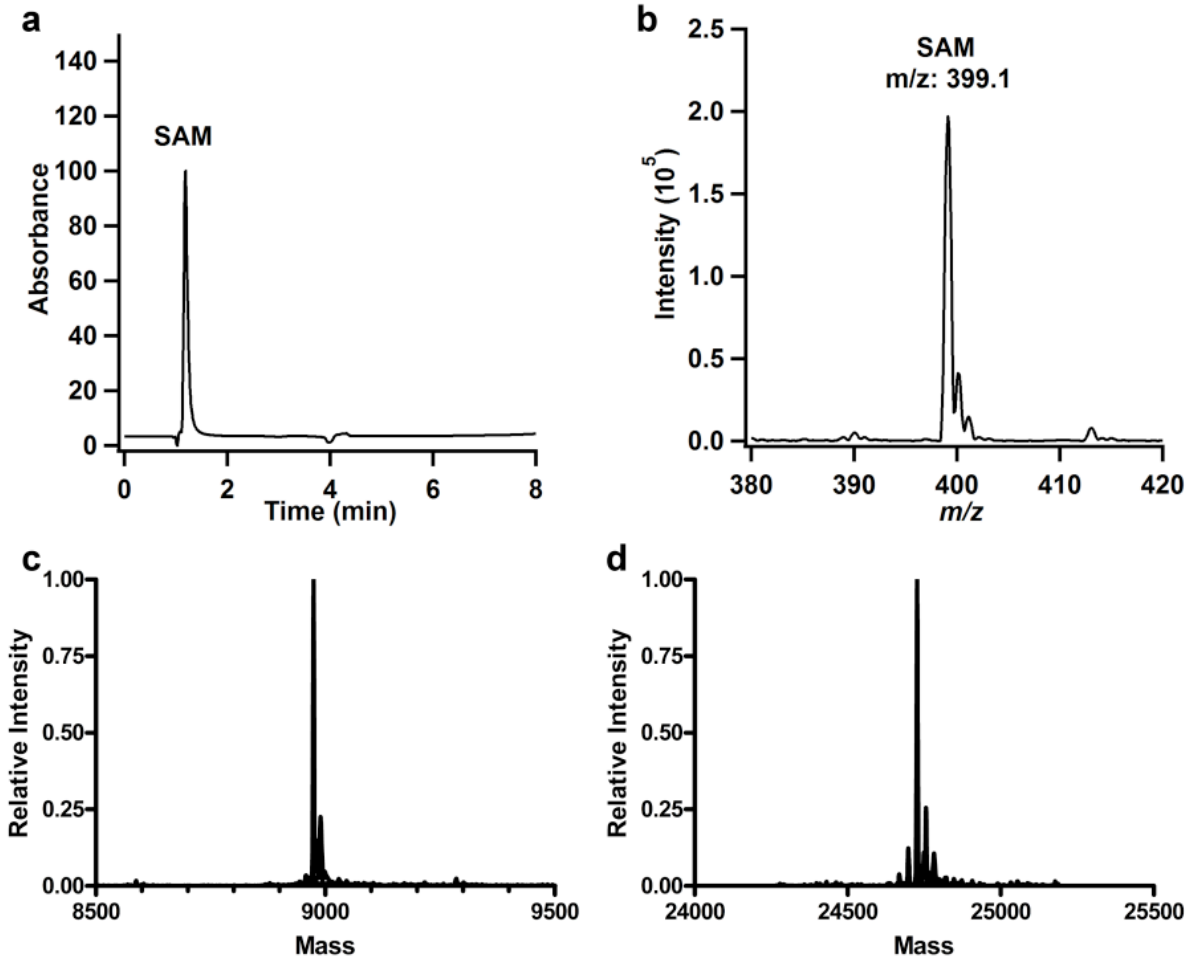

Figure S5: Purity analyses of substrates and BmaI1 preparations. (a) Relative absorbance at 260 nm for pure SAM separated by HPLC. (b) Mass spectrum of SAM. (c) The deconvoluted mass spectrum of C8-ACP. The experimentally determined mass was 8,974 Da and the theoretical was 8,973 Da. d) The deconvoluted mass spectrum of His-BmaI1. BmaI1 has a theoretical mass of 24,722 Da and a measured mass of 24,727 as determined by electrospray mass spectrometry.

Table S1: Strains, plasmids, and primers

***E. coli* Strains**	**Relevant Characteristics**	**Source**
BW25113	Δ*(araD-araB)567*, Δ*lacZ4787*(::rrnB-3), λ⁻, *rph-1*, Δ*(rhaD-rhaB)568*, *hsdR514*	(8)
Tuner DE3	F⁻ *ompT gal dcm lon hsdS*$_B$(r_B^- m_B^-) λ(DE3 [*lacI lacUV5*-T7 gene 1 *ind1 sam7 nin5*])	Merck
JT-apo	(DK574 pJT94) F⁻ *metB1 relA1 spoT1 gyrA216 panD2 zad-220*::Tn10, pMS421, pMR19, pJT94	(2)
QC306	Tuner DE3	This study
QC373	Tuner DE3	This study
QC384	BW25113	This study
Plasmids		
pBD2	*bmal1* under arabinose control	(9)
pMCSG21	cloning vector	(10)
pMCSG23	cloning vector	(10)
pQC201	pMCSG21 expressing His-Bmal1 by a T7 promoter	This study
pQC218	pMCSG23 expressing MBP-YspI by a T7 promoter	This study
Primers		
bmal1 foward	TACTTCCAATCCAATGCGCGAACTTTCGTTCATGGCGACG	
bmal1 reverse	TTATCCACTTCCAATGTTATCAGGCGGCTTCGGCGG	
yspI forward	TACTTCCAATCCAATGCGTTAGAAATTTTCGATGTCAG	
yspI reverse	TTATCCACTTCCAATGTTATTAAGCCGATTCTGGCATAACGGG	

Table S2: Compound properties calculated by using ADMETpredictor (Simulations Plus, Lancaster, PA)

Compound	**1**	**3**	**5**
Octanol-water coefficient (logP)	3.8	2.4	-1.7
Effective intestinal permeability (Peff)	3.7	1.3	0.4
Solubility in water (mg/ml)	0.1	0.2	8.9
% Unbound to blood protein	8.0	9.8	47.7